The Journal of Laryngology & Otology

cambridge.org/jlo

# Arterial spin labelling and diffusion-weighted magnetic resonance imaging in differentiation of recurrent head and neck cancer from post-radiation changes

A A K Abdel Razek

Department of Diagnostic Radiology, Faculty of Medicine, Mansoura University, Egypt

## Main Article

Dr A A K Abdel Razek takes responsibility for the integrity of the content of the paper

**Cite this article:** Abdel Razek AAK. Arterial spin labelling and diffusion-weighted magnetic resonance imaging in differentiation of recurrent head and neck cancer from post-radiation changes. *J Laryngol Otol* 2018; **132**:923–928. https://doi.org/10.1017/S0022215118001743

Accepted: 4 April 2018

**Key words:**
Neoplasms; Recurrence; Radiotherapy

**Author for correspondence:**
Dr Ahmed Abdel Khalek Abdel Razek, Department of Diagnostic Radiology, Faculty of Medicine, Mansoura University, Mansoura 13351, Egypt
E-mail: arazek@mans.edu.eg
Fax: +20 502 315 105

## Abstract

**Objective.** To assess arterial spin labelling and diffusion-weighted imaging in the differentiation of recurrent head and neck cancer from post-radiation changes.

**Methods.** A retrospective study was conducted of 47 patients with head and neck cancer, treated with radiotherapy, who underwent magnetic resonance arterial spin labelling and diffusion-weighted magnetic resonance imaging. Tumour blood flow and apparent diffusion co-efficient of the lesion were calculated.

**Results.** There was significant difference ($p = 0.001$) in tumour blood flow between patients with recurrent head and neck cancer ($n = 31$) ($47.37 \pm 16.3$ ml/100 g/minute) and those with post-radiation changes ($n = 16$) ($18.80 \pm 2.9$ ml/100 g/minute). The thresholds of tumour blood flow and apparent diffusion co-efficient used for differentiating recurrence from post-radiation changes were more than 24.0 ml/100 g/minute and $1.21 \times 10^{-3}$ $mm^2$/second or less, with area under the curve values of 0.94 and 0.90, and accuracy rates of 88.2 per cent and 88.2 per cent, respectively. The combined tumour blood flow and apparent diffusion co-efficient values used for differentiating recurrence from post-radiation changes had an area under the curve of 0.96 and an accuracy of 90.2 per cent.

**Conclusion.** Combined tumour blood flow and apparent diffusion co-efficient can differentiate recurrence from post-radiation changes.

## Introduction

Interpretation of head and neck cancer after radiotherapy is difficult because radiotherapy and chemotherapy can result in oedema and fibrosis that can mimic tumour recurrence.[1–4] Differentiation between residual or recurrent tumour and post-radiation fibrosis is difficult with routine computed tomography (CT) and magnetic resonance imaging (MRI).[2–6] Dynamic contrast MRI, dynamic susceptibility contrast perfusion-weighted MRI and proton magnetic resonance spectroscopy are used in the differentiation of recurrent head and neck cancer from post-radiation changes, but their parameters overlap.[6–11] Contrast CT and perfusion CT are associated with the administration of contrast medium and radiation exposure.[12,13] Positron emission tomography (PET)/CT and PET/MRI are not routinely available and are expensive.[14,15] Biopsy is the 'gold standard' for assessing a post-radiation neck, but the findings may be inconclusive or the sample inadequate.[1–4]

Arterial spin labelling perfusion-weighted MRI allows for quantitative mapping of tissue perfusion, without the use of contrast agents. The magnetisation of arterial blood water is labelled by magnetic inversion or saturation, and the delivery of labelled blood water to tissues is observed.[16,17] A few recent studies have discussed the role of arterial spin labelling in head and neck cancer.[17–20] The pseudo-continuous arterial spin labelling is a variant of continuous arterial spin labelling, which utilises a series of discrete radiofrequency pulses to mimic the continuous arterial spin labelling method for spin labelling. The pseudo-continuous arterial spin labelling parameter of tumour blood flow reflects physiological information about tissue perfusion.[17–19]

Diffusion-weighted MRI is based on Brownian motion of water protons in the tissue, which are affected by the microstructure of tissue. Some previous studies have assessed diffusion-weighted MRI for differentiating and characterising primary head and neck tumours, and investigated its usefulness in discriminating between recurrent or residual tumour and post-radiation changes.[20–26]

This study aimed to assess arterial spin labelling and diffusion-weighted MRI in the differentiation of recurrent head and neck cancer from post-radiation changes.

## Materials and methods

### *Patients*

Institutional Review Board approval was obtained; the requirement for patients' informed consent was waived for this retrospective study.

The study included 49 consecutive patients with head and neck squamous cell carcinoma. All the patients included had completed a course of radiotherapy but had suspected recurrence clinically, and all had undergone imaging three months after treatment. Two patients were excluded from the study because of motion artefacts on MRI.

The images of 47 patients (33 males and 14 females), aged 52–74 years (mean age of 65 years), were evaluated. The sites of suspected recurrence were located in: the nasal cavity and paranasal sinuses ($n = 27$), the oropharynx ($n = 11$), and the oral cavity ($n = 9$). The final diagnosis was determined using surgical biopsy ($n = 25$), fine needle aspiration biopsy ($n = 13$) and core biopsy ($n = 9$).

### Routine magnetic resonance imaging

All MRI scans were acquired on a 1.5 Tesla scanner (Ingenia; Philips Medical Systems, Best, the Netherlands) with a 16-channel neurovascular coil. T1-weighted images (repetition time/echo time = 800/15 ms) and T2-weighted fast spin-echo images (repetition time/echo time = 6000/80 ms) were acquired for all patients. The scanning parameters were: section thickness = 5 mm, interslice gap = 1.5 mm, field of view = 25–30 $cm^2$, and acquisition matrix = 256 × 224. Coronal T2-weighted imaging was performed to a defined location of carotid artery bifurcation for the positioning of the labelling slab in pseudo-continuous arterial spin labelling. Post-contrast T1-weighted images were obtained after arterial spin labelling and diffusion-weighted MRI, using the same parameters as for pre-contrast T1-weighted images.

### Diffusion-weighted magnetic resonance imaging

Diffusion-weighted MRI scans were obtained using a multi-slice, single-shot, spin-echo, echo-planar image sequence. Chemical shift selective fat-suppression was used to reduce diffusion-weighted MRI scan artefacts. The motion-probing gradient was applied before and after the 180-degree pulse with echo-planar imaging readout. The imaging parameters were: repetition time/echo time = 10 000/108 ms, number of excitations = 16, bandwidth = 300 kHz, field of view = 25–30 $cm^2$, section thickness = 5 mm, interslice gap = 1 mm, and acquisition matrix = 256 × 128. The diffusion gradients were applied in three orthogonal directions (Y, X and Z). The diffusion-weighted MRI scans were acquired with b-values of 0, 500 and 1000 $s/mm^2$, and the apparent diffusion co-efficient maps were reconstructed.

### Arterial spin labelling

Pseudo-continuous arterial spin labelling was performed using single-phase arterial spin labelling, with a fast field echo-planar imaging sequence, to obtain control images and labelled images. The patients were instructed not to swallow, move their tongue or open their mouth during the scanning. The scanning parameters were: labelling duration = 1650 ms, post-label delay = 1280 ms, repetition time/echo time = 400/20 ms, flip angle = 35 degrees, slice thickness = 6 mm, interslice gap = 0.6 mm, field of view = 25 cm × 20 cm, sensitivity encoding ('SENSE') factor = 2.5, and scanning time = 4 minutes and 20 seconds. The labelling plane was located at the level of the common carotid artery, just below the bifurcation. A T1-weighted map was obtained to measure the longitudinal relaxation in the tumour tissue.

### Image analysis

Image analysis was performed by a radiologist with 20 years of MRI experience (author AAK Abdel Razek), who was blinded to the clinical data and pathological results. The labelled images were subtracted from the control images to obtain a set of new subtracted images. A region of interest was placed on the subtracted image around the suspicious lesion, avoiding cystic and necrotic regions, using an electronic cursor (Figure 1). The tumour blood flow was calculated using a previously described equation.[18] A copy of the region of interest was placed on the apparent diffusion co-efficient map.

### Statistical analysis

The statistical analysis of data was conducted using SPSS software version 16.0 (SPSS, Chicago, Illinois, USA). The mean and standard deviation values for tumour blood flow and apparent diffusion co-efficient, for recurrent head and neck cancer and post-radiation changes, were calculated. The data were analysed to determine statistically significant differences. The student's *t*-test was used to compare the tumour blood flow and apparent diffusion co-efficient values for recurrent cancer and post-radiation changes. A *p*-value of less than 0.05 was considered statistically significant. The receiver operating characteristic curve results for tumour blood flow, apparent diffusion co-efficient, and combined tumour blood flow and apparent diffusion co-efficient were used to differentiate recurrence from post-radiation changes, calculating the area under the curve, accuracy, sensitivity, specificity, and positive and negative predictive values.

## Results

Table 1 shows the means, standard deviations and ranges of tumour blood flow (ml/100 g/minute) and apparent diffusion co-efficient ($\times 10^{-3}$ $mm^2$/second) values for recurrent head and neck cancer and post-radiation changes.

The tumour blood flow for patients with recurrent head and neck cancer ($n = 31$) ranged from 21.0 to 77.0 ml/100 g/minute, with a mean value of 47.37 ± 16.3 ml/100 g/minute. The tumour blood flow for patients with post-radiation changes ($n = 16$) ranged from 13.0 to 25.0 ml/100 g/minute, with a mean value of 18.80 ± 2.9 ml/100 g/minute. The difference in tumour blood flow between recurrent tumour and post-radiation changes was statistically significant ($p = 0.001$). The best results were obtained when a tumour blood flow value of more than 24.0 ml/100 g/minute was used for differentiating tumour recurrence from post-radiation changes, with an area under the curve of 0.94, accuracy of 88.2 per cent, sensitivity of 85.7 per cent, specificity of 93.8 per cent, a positive predictive value of 96.8 per cent and a negative predictive value of 75.0 per cent (Table 2 and Figure 2).

The apparent diffusion co-efficient for patients with recurrent tumours ranged from 0.94 to $1.42 \times 10^{-3}$ $mm^2$/second, with a mean value of $1.11 \pm 0.1 \times 10^{-3}$ $mm^2$/second. The apparent diffusion co-efficient for patients with post-radiation changes ranged from 1.38 to $1.59 \times 10^{-3}$ $mm^2$/second, with a mean value of $1.49 \pm 0.1 \times 10^{-3}$ $mm^2$/second. The difference between the apparent diffusion co-efficient values for recurrent tumour and post-radiation changes was statistically significant ($p = 0.001$). When an apparent diffusion co-efficient value of $1.21 \times 10^{-3}$ $mm^2$/second or less was used as the cut-off value for differentiating recurrence from post-radiation

https://doi.org/10.1017/S0022215118001743 Published online by Cambridge University Press

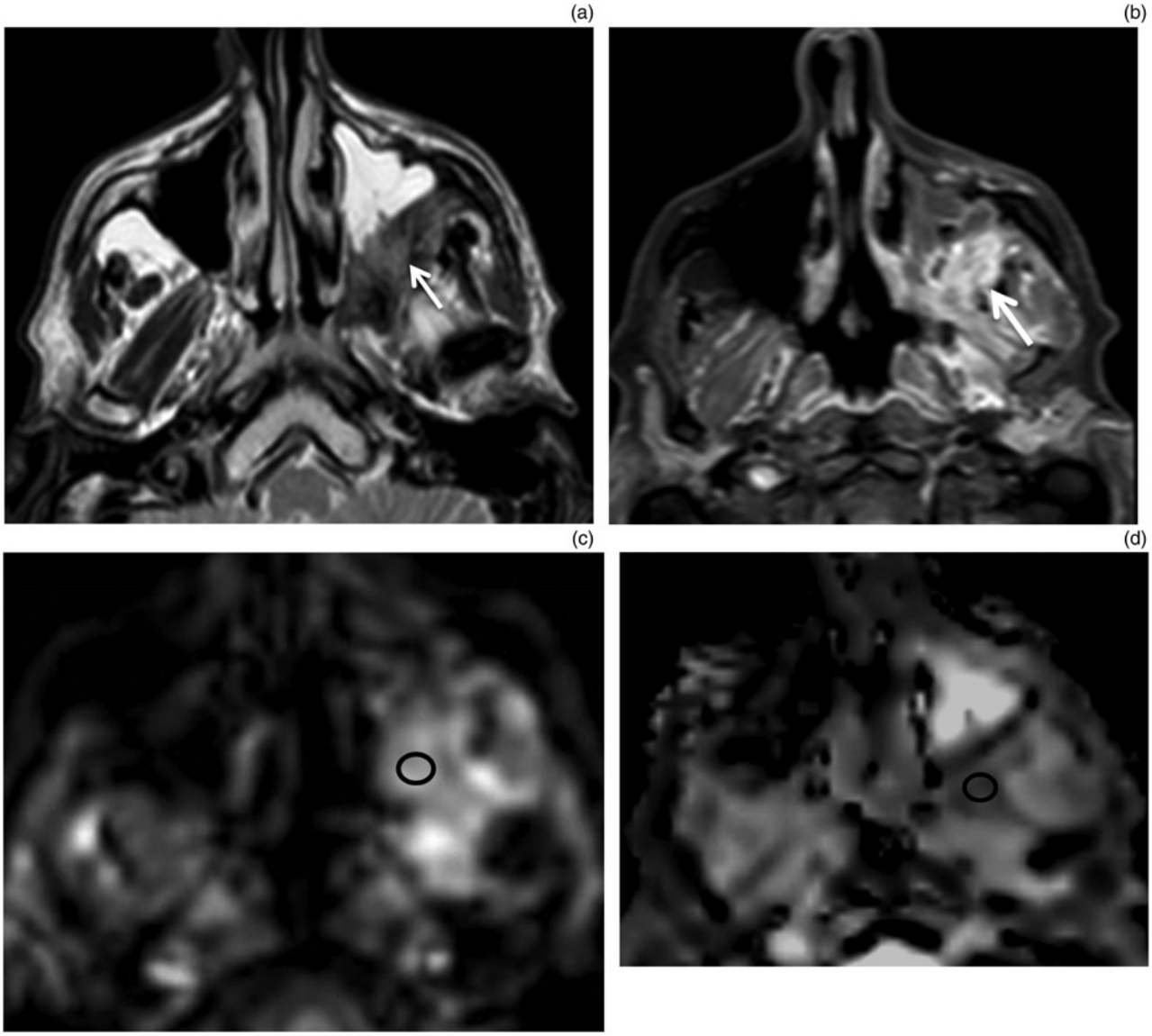


**Fig. 1.** Recurrent head and neck cancer after radiotherapy. (a) Axial T2-weighted magnetic resonance imaging (MRI) scan shows hypointense lesion (arrow) along the postero-lateral wall of the left maxillary sinus. (b) Axial contrast T1-weighted MRI scan shows mild inhomogeneous enhancement of the lesion (arrow). (c) Axial arterial spin labelling map shows localisation of the region of interest within the lesion. (d) Axial apparent diffusion co-efficient map shows restricted diffusion with a low apparent diffusion co-efficient value ($0.91 \times 10^{-3}$ mm$^2$/second) for the recurrent cancer.

**Table 1.** Tumour blood flow and apparent diffusion co-efficient values for recurrent head and neck cancer and post-radiation changes

| Parameter | Recurrent cancer* | Post-radiation changes† | *P*-value |
|---|---|---|---|
| TBF (mean ± SD (range); ml/100 g/minute) | 47.37 ± 16.3 (21.0–77.0) | 18.80 ± 2.9 (13.0–25.0) | 0.001 |
| ADC (mean ± SD (range); × $10^{-3}$ mm$^2$/second) | 1.11 ± 0.1 (0.94–1.42) | 1.49 ± 0.1 (1.38–1.59) | 0.001 |

*$n$ = 31; †$n$ = 16. TBF = tumour blood flow; SD = standard deviation; ADC = apparent diffusion co-efficient

changes, the area under the curve was 0.90, accuracy was 88.2 per cent, sensitivity was 91.4 per cent, specificity was 81.2 per cent, the positive predictive value was 91.4 per cent and the negative predictive value was 81.2 per cent (Table 2 and Figure 2).

The combination of a tumour blood flow value of 24.0 ml/100 g/minute and an apparent diffusion co-efficient value of $1.21 \times 10^{-3}$ mm$^2$/second was used as a cut-off value for the differentiation of recurrence from post-radiation changes, with an area under the curve of 0.96, accuracy of 90.2 per cent, sensitivity of 88.6 per cent, specificity of 93.8 per cent, a positive predictive value of 96.9 per cent and a negative predictive value of 78.9 per cent (Table 2 and Figure 2).

## Discussion

In this study, the main finding was that arterial spin labelling can be used for assessing head and neck cancer after treatment. Recurrent head and neck cancer was associated with higher tumour blood flow and restricted diffusion, with a reduced apparent diffusion co-efficient. In comparison, post-radiation changes were associated with lower tumour blood flow and no significant restriction in diffusion.

In this study, the tumour blood flow for recurrent head and neck cancer was significantly different to that for post-radiation changes. This is attributed to increased vascularity with increased capillary perfusion in recurrent or residual tumours compared to post-radiation changes. The tumour

https://doi.org/10.1017/S0022215118001743 Published online by Cambridge University Press

**Table 2.** Receiver operating characteristic curve results of tumour blood flow and apparent diffusion co-efficient for recurrent head and neck cancer versus post-radiation changes

| Parameter | Cut-off point | AUC | Sensitivity | Specificity | PPV | NPV | Accuracy |
|---|---|---|---|---|---|---|---|
| TBF (ml/100 g/minute) | 24.0 | 0.94 | 85.7 | 93.8 | 96.8 | 75.0 | 88.2 |
| ADC ($\times 10^{-3}$ $mm^2$/second) | 1.21 | 0.90 | 91.4 | 81.2 | 91.4 | 81.2 | 88.2 |
| Combined | | 0.96 | 88.6 | 93.8 | 96.9 | 78.9 | 90.2 |

AUC = area under the curve; PPV = positive predictive value; NPV = negative predictive value; TBF = tumour blood flow; ADC = apparent diffusion co-efficient

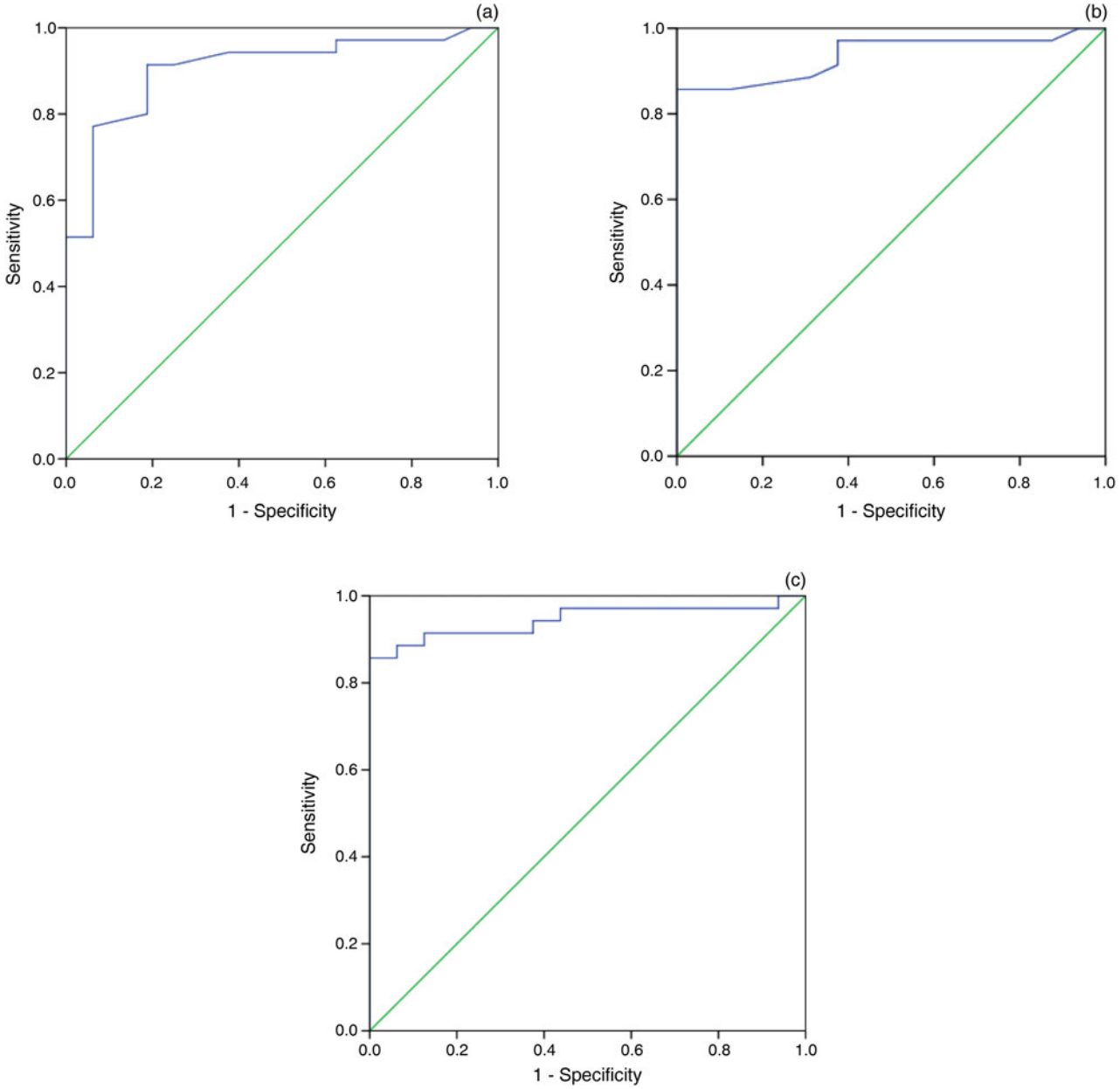


**Fig. 2.** Receiver operating characteristic curve results for (a) apparent diffusion co-efficient, (b) tumour blood flow, and (c) combined apparent diffusion co-efficient and tumour blood flow values, used to differentiate recurrent head and neck cancer from post-radiation changes (the diagonal segments are produced by ties). (The thresholds used are detailed in the main text.)

blood vessels are typically dilated and tortuous, with an abnormal branching pattern, dead ends, and no organisation into arterioles, capillaries and venules.[16,17] One study reported that tumour blood flow can be useful for determining local control, and the combined use of the percentage change of tumour blood flow and tumour volume had particularly high diagnostic accuracy.[18] Another study showed that pre- and post-radiation tumour blood flow differed significantly.[19] Post-radiation tumour blood flow was significantly higher in patients with residual tumours than in those without. The tumour blood flow reduction rate was significantly lower in patients with residual tumours than in those without.[19]

In this study, the apparent diffusion co-efficient for recurrent head and neck cancer was lower than that for post-radiation changes. Recurrent head and neck cancer showed restricted diffusion, with a low apparent diffusion co-efficient

https://doi.org/10.1017/S0022215118001743 Published online by Cambridge University Press

compared with radio-necrosis, presumably due to increased free water in necrosis and increased cellularity in recurrent tumours.[21,22] As diffusion within recurrent or residual tumours is impeded by the presence of cellular membranes and macromolecular structures, treatment with radiation and/or chemotherapy triggers cell death that can result in the loss of cell membrane integrity and reduced cell density, which can be detected as an increased mean diffusion value for the tumour.[23,24] One study reported that the apparent diffusion co-efficient value for residual or recurrent tumours was significantly lower than that of post-radiation changes.[24] Another study found that bi-exponential fitting of the apparent diffusion co-efficient values on diffusion-weighted MRI were significantly lower in patients with residual tumours compared to those without tumour.[25] Lastly, advanced diffusion fitting models such as diffusion kurtosis imaging and the stretched exponential model are the diagnostic tools for detecting residual tumours in post-treatment granulation.[26]

In this study, combined tumour blood flow and apparent diffusion co-efficient values increased the diagnostic accuracy of MRI in the differentiation of recurrent head and neck cancer from post-radiation changes. A few studies have suggested that multi-parametric MRI, with the calculation of different biomarkers of diffusion and perfusion parameters, may help in differentiating recurrence from post-radiation changes.[27–29]

- There was a significant difference ($p = 0.001$) in tumour blood flow between recurrent head and neck cancer and post-radiation changes
- There was a significant difference ($p = 0.001$) in apparent diffusion co-efficient between recurrent head and neck cancer and post-radiation changes
- Arterial spin labelling is a non-invasive imaging method for assessing head and neck cancer after radiotherapy
- Combined tumour blood flow and apparent diffusion co-efficient values can predict head and neck cancer recurrence after radiotherapy

There are a few limitations to this study. First, there was no follow up of patients. Further studies, which monitor patients after radiotherapy, are recommended. Second, we utilised the calculation of tumour blood flow. Applications of advanced post-processing techniques for tumour blood flow, with the creation of parametric blood flow maps, and use of diffusion tensor imaging or kurtosis imaging, will improve the results.[26,30–36]

## Conclusion

The combination of tumour blood flow and apparent diffusion co-efficient values can play a role in differentiating recurrent head and neck cancer from post-radiation changes.

**Competing interests.** None declared

## References


1 Chang JH, Wu CC, Yuan KS, Wu AT, Wu SY. Locoregionally recurrent head and neck squamous cell carcinoma: incidence, survival, prognostic factors, and treatment outcomes. *Oncotarget* 2017;**8**:55600–12

2 Shaikh T, Handorf EA, Murphy CT, Mehra R, Ridge JA, Galloway TJ. The impact of radiation treatment time on survival in patients with head and neck cancer. *Int J Radiat Oncol Biol Phys* 2016;**96**:967–75

3 Abdel Razek A. Neoplastic pathology of the neck. In Luca S, ed. *Image Principles, Neck, and the Brain*. Boca Raton, FL: CRC Press, 2016;425–52

4 Saito N, Nadgir RN, Nakahira M, Takahashi M, Uchino A, Kimura F *et al.* Posttreatment CT and MR imaging in head and neck cancer: what the radiologist needs to know. *Radiographics* 2012;**32**:1261–82

5 King AD, Keung CK, Yu KH, Mo FK, Bhatia KS, Yeung DK *et al.* T2-weighted MR imaging early after chemoradiotherapy to evaluate treatment response in head and neck squamous cell carcinoma. *AJNR Am J Neuroradiol* 2013;**34**:1237–41

6 Chikui T, Kawano S, Kawazu T, Hatakenaka M, Koga S, Ohga M *et al.* Prediction and monitoring of the response to chemoradiotherapy in oral squamous cell carcinomas using a pharmacokinetic analysis based on the dynamic contrast-enhanced MR imaging findings. *Eur Radiol* 2011;**21**:1699–708

7 Abdel Razek AA, Gaballa G, Ashamalla G, Alashry MS, Nada N. Dynamic susceptibility contrast perfusion-weighted MR imaging and diffusion-weighted MR imaging in differentiating recurrent head and neck cancer from post-radiation changes. *J Comput Assist Tomogr* 2015;**39**:849–54

8 Abdel Razek AA, Gaballa G. Role of perfusion magnetic resonance imaging in cervical lymphadenopathy. *J Comput Assist Tomogr* 2011;**35**:21–5

9 King AD, Yeung DK, Yu KH, Mo FK, Hu CW, Bhatia KS *et al.* Monitoring of treatment response after chemoradiotherapy for head and neck cancer using in vivo 1H MR spectroscopy. *Eur Radiol* 2010;**20**:165–72

10 Razek AA, Nada N. Correlation of choline/creatine and apparent diffusion coefficient values with the prognostic parameters of head and neck squamous cell carcinoma. *NMR Biomed* 2016;**29**:483–9

11 Abdel Razek AA, Poptani H. MR spectroscopy of head and neck cancer. *Eur J Radiol* 2013;**82**:982–9

12 Clavel S, Charron MP, Bélair M, Delouya G, Fortin B, Després P *et al.* The role of computed tomography in the management of the neck after chemoradiotherapy in patients with head-and-neck cancer. *Int J Radiat Oncol Biol Phys* 2012;**82**:567–73

13 Razek AA, Tawfik A, Elsorogy L, Soliman N. Perfusion CT of head and neck cancer. *Eur J Radiol* 2014;**83**:537–44

14 Kostakoglu L, Fardanesh R, Posner M, Som P, Rao S, Park E *et al.* Early detection of recurrent disease by FDG-PET/CT leads to management changes in patients with squamous cell cancer of the head and neck. *Oncologist* 2013;**18**:1108–17

15 Lee YZ, Ramalho J, Kessler B. PET-MR imaging in head and neck. *Magn Reson Imaging Clin N Am* 2017;**25**:315–24

16 Razek AA, El-Serougy L, Abdelsalam M, Gaballa G, Talaat M. Differentiation of residual/recurrent gliomas from postradiation necrosis with arterial spin labeling and diffusion tensor magnetic resonance imaging-derived metrics. *Neuroradiology* 2018;**60**:169–77

17 Fujima N, Kudo K, Tsukahara A, Yoshida D, Sakashita T, Homma A *et al.* Measurement of tumor blood flow in head and neck squamous cell carcinoma by pseudo-continuous arterial spin labeling: comparison with dynamic contrast-enhanced MRI. *J Magn Reson Imaging* 2015;**41**:983–91

18 Fujima N, Yoshida D, Sakashita T, Homma A, Tsukahara A, Tha KK *et al.* Usefulness of pseudocontinuous arterial spin-labeling for the assessment of patients with head and neck squamous cell carcinoma by measuring tumor blood flow in the pretreatment and early treatment period. *AJNR Am J Neuroradiol* 2016;**37**:342–8

19 Fujima N, Kudo K, Yoshida D, Homma A, Sakashita T, Tsukahara A *et al.* Arterial spin labeling to determine tumor viability in head and neck cancer before and after treatment. *J Magn Reson Imaging* 2014;**40**:920–8

20 Razek AA. Assessment of masses of the external ear with diffusion-weighted MR imaging. *Otol Neurotol* 2018;**39**:227–31

21 Abdel Razek AA. Assessment of solid lesions of the temporal fossa with diffusion-weighted magnetic resonance imaging. *Int J Oral Maxillofac Surg* 2015;**44**:1081–5

22 Varoquaux A, Rager O, Dulguerov P, Burkhardt K, Ailianou A, Becker M. Diffusion-weighted and PET/MR imaging after radiation therapy for malignant head and neck tumor. *Radiographics* 2015;**35**:1502–27

23 Hwang I, Choi SH, Kim YJ, Kim KG, Lee AL, Yun TJ *et al.* Differentiation of recurrent tumor and posttreatment changes in head and neck squamous cell carcinoma: application of high b-value diffusion-weighted imaging. *AJNR Am J Neuroradiol* 2013;**34**:2343–8

24 Abdel Razek AA, Kandeel AY, Soliman N, El-shenshawy HM, Kamel Y, Nada N *et al.* Role of diffusion-weighted echo-planar MR imaging in


https://doi.org/10.1017/S0022215118001743 Published online by Cambridge University Press

differentiation of residual or recurrent head and neck tumors and post-treatment changes. *AJNR Am J Neuroradiol* 2007;**28**:1146–52
25 Hauser T, Essig M, Jensen A, Laun FB, Münter M, Maier-Hein KH *et al.* Prediction of treatment response in head and neck carcinomas using IVIM-DWI: evaluation of lymph node metastasis. *Eur J Radiol* 2014;**83**:783–7
26 Fujima N, Yoshida D, Sakashita T, Homma A, Kudo K, Shirato H. Residual tumour detection in post-treatment granulation tissue by using advanced diffusion models in head and neck squamous cell carcinoma patients. *Eur J Radiol* 2017;**90**:14–19
27 Min M, Lee MT, Lin P, Holloway L, Wijesekera D, Gooneratne D *et al.* Assessment of serial multi-parametric functional MRI (diffusion-weighted imaging and R2*) with (18)F-FDG-PET in patients with head and neck cancer treated with radiation therapy. *Br J Radiol* 2016;**89**:20150530
28 Wong KH, Panek R, Bhide SA, Nutting CM, Harrington KJ, Newbold KL. The emerging potential of magnetic resonance imaging in personalizing radiotherapy for head and neck cancer: an oncologist's perspective. *Br J Radiol* 2017;**90**:20160768
29 King AD, Thoeny HC. Functional MRI for the prediction of treatment response in head and neck squamous cell carcinoma: potential and limitations. *Cancer Imaging* 2016;**16**:23
30 Abdel Razek A, Elkhamary S, Al-Mesfer S, Alkatan HM. Correlation of apparent diffusion coefficient at 3 T with prognostic parameters of retinoblastoma. *AJNR Am J Neuroradiol* 2012;**33**:944–8
31 Tawfik AM, Razek AA, Kerl JM, Nour-Eldin NE, Bauer R, Vogl TJ. Comparison of dual-energy CT-derived iodine content and iodine overlay of normal, inflammatory and metastatic squamous cell carcinoma cervical lymph nodes. *Eur Radiol* 2014;**24**:574–80
32 Abdel Razek AA, Gaballa G. Role of perfusion magnetic resonance imaging in cervical lymphadenopathy. *J Comput Assist Tomogr* 2011;**35**:21–5
33 Abdel Razek AA, Samir S, Ashmalla GA. Characterization of parotid tumors with dynamic susceptibility contrast perfusion-weighted magnetic resonance imaging and diffusion-weighted MR imaging. *J Comput Assist Tomogr* 2017;**41**:131–6
34 Razek AA, Sieza S, Maha B. Assessment of nasal and paranasal sinus masses by diffusion-weighted MR imaging. *J Neuroradiol* 2009;**36**:206–11
35 El-Serougy L, Abdel Razek AA, Ezzat A, Eldawoody H, El-Morsy A. Assessment of diffusion tensor imaging metrics in differentiating low-grade from high-grade gliomas. *Neuroradiol J* 2016;**29**:400–7
36 Razek AA. Prediction of malignancy of submandibular gland tumors with apparent diffusion coefficient. *Oral Radiol* 2017; doi.org/10.1007/s11282-017-0311-y

https://doi.org/10.1017/S0022215118001743 Published online by Cambridge University Press